

Tomographic refractive index profiling of direct laser written waveguides: supplement

NICOLAS BARRÉ,^{1,*} RAVI SHIVARAMAN,² LISA ACKERMANN,^{3,4}  SIMON MOSER,¹ MICHAEL SCHMIDT,^{3,4}  PATRICK SALTER,²  MARTIN BOOTH,^{2,4}  AND ALEXANDER JESACHER^{1,4} 

¹*Institute of Biomedical Physics, Medical University of Innsbruck, Müllerstraße 44, 6020 Innsbruck, Austria*

²*Department of Engineering Science, University of Oxford, Parks Road, Oxford OX1 3PJ, UK*

³*Institute of Photonic Technologies, Friedrich-Alexander-University Erlangen-Nürnberg, Konrad-Zuse-Straße 3/5, Erlangen 91052, Germany*

⁴*Erlangen Graduate School in Advanced Optical Technologies (SAOT), Friedrich-Alexander-University Erlangen-Nürnberg, Paul-Gordan-Straße 6, 91052 Erlangen, Germany*

**nicolas.barre@i-med.ac.at*

This supplement published with Optica Publishing Group on 14 October 2021 by The Authors under the terms of the [Creative Commons Attribution 4.0 License](https://creativecommons.org/licenses/by/4.0/) in the format provided by the authors and unedited. Further distribution of this work must maintain attribution to the author(s) and the published article's title, journal citation, and DOI.

Supplement DOI: <https://doi.org/10.6084/m9.figshare.16635577>

Parent Article DOI: <https://doi.org/10.1364/OE.434846>

Tomographic refractive index profiling of direct laser written waveguides: supplemental document

We provide a detailed schematic of our imaging setup and describe the tomography algorithm we developed in order to reconstruct the 2D refractive index (RI) profiles associated to shift-invariant laser written waveguides. We first describe the forward model from which we obtain the intensity images to compare to the experimental data. Then, we derive the gradient expression associated with our error metric by following a backpropagation scheme. Finally, we present the proximal gradient descent we use for the reconstruction.

1. TOMOGRAPHY SETUP

Figure S1 shows a detailed sketch of our tomography setup. Light from a blue LED is focused onto a pinhole of $150\ \mu\text{m}$ diameter and collimated by a lens of $200\ \text{mm}$ focal length. The light is reflected off a motorized mirror at a user definable angle. The beam is then focused into the condenser back aperture (CBA), where it forms a slightly demagnified image of the pinhole. The lateral position of the pinhole image in the CBA defines the angle of illumination in the focal plane (FP).

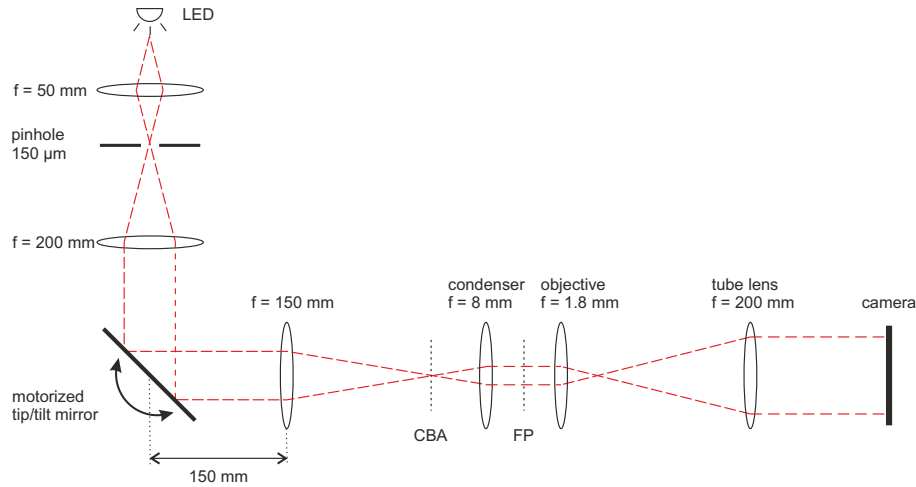


Fig. S1. Layout of our optical tomography setup. CBA = condenser back aperture; FP = focal plane.

2. FORWARD MODEL

The recorded experimental data consists of a set of N intensity images denoted $I_{\text{exp}}^{(k)}$, corresponding to intensity diffraction patterns of tilted plane waves with angles $\{\theta_k\}_{1 \leq k \leq N}$ sent across the sample. In the particular case of the shift-invariant waveguides we are dealing with, the recorded intensities $I_{\text{exp}}^{(k)}$ are assumed to be 1-dimensional. As already stated in the main text, these 1-dimensional views are obtained from the 2D camera images by averaging over a hundred pixels along the invariant direction of the considered waveguide.

In order to reconstruct the unknown RI profile, we first need to define a forward model which takes a tilted plane wave with angle θ_k as an input, and outputs a 1D intensity image $I_{\text{sim}}^{(k)}$ to be compared to $I_{\text{exp}}^{(k)}$. This forward model takes the RI profile and the aberration correction as parameters, on which a joint optimization will be performed later.

A. Propagation model

We consider the propagation of tilted plane waves across a medium $\text{RI}(x, z) = n_0 + \Delta\text{RI}(x, z)$, where n_0 is the refractive index of the bulk glass at the wavelength λ , and $\Delta\text{RI}(x, z)$ is the RI change induced by the laser writing process. The direction x corresponds to the camera imaging plane whereas the orthogonal direction z defines the optical axis of the imaging system. The propagation angle $\theta = 0$ corresponds to straight illumination.

We model the propagation through such medium thanks to the well known split-step Fourier Beam Propagation Method (BPM) [1], to which we make two important changes. First, in order to avoid Fourier issues due to wrong wrapping over the field boundaries, we integrate the information about the wave angle θ_k into the propagator instead of the wave field E_k . Second, in order to be more accurate when propagating to large angles, we re-scale the phase contributions of the thin medium slices according to the cosine of the angle of the incoming wave, as justified in [2].

More formally, we define the propagation of an incoming wave E_k with angle θ_k in an homogeneous medium n_0 of thickness z by the operator:

$$\mathcal{P}_z(E_k) = \mathcal{F}^{-1} \left(\mathcal{F}(E_k) \exp \left(i2\pi z \sqrt{\frac{n_0^2}{\lambda^2} - \left(f_x - \frac{n_0 \sin \theta_k}{\lambda} \right)^2} \right) \right). \quad (\text{S1})$$

Moreover, at a given transverse position $z = cst$, the phase contribution of a thin slice of differential refractive index ΔRI with thickness Δz is modeled by the operator:

$$\mathcal{N}_{\Delta\text{RI}}(E_k) = E_k \exp \left(i \frac{2\pi}{\lambda} \Delta z \frac{\Delta\text{RI}}{\cos \theta_k} \right). \quad (\text{S2})$$

This allows to define the propagation through a thin slice ΔRI with thickness Δz as the composition of the previous operators:

$$\mathcal{P}_{\Delta\text{RI}} = \mathcal{P}_{\frac{\Delta z}{2}} \circ \mathcal{N}_{\Delta\text{RI}} \circ \mathcal{P}_{\frac{\Delta z}{2}}. \quad (\text{S3})$$

With this approach, we have to set $E_k(x)|_{z=0} = 1$, whatever the incoming propagation angle. Then, a sample of total thickness L_z needs to be split into N_l layers satisfying $L_z = N_l \Delta z$, so that the final field distribution $E_k(x)|_{z=L_z}$ can be obtained by successive applications of the propagator $\mathcal{P}_{\Delta\text{RI}}$ (S3). Without taking aberration correction into account, the result of the forward model is:

$$I_{\text{sim}}^{(k)} = \left| \mathcal{P}_{\Delta\text{RI}}^{(N_l)} \left(E_k|_{z=0} \right) \right|^2 = \left| E_k|_{z=L_z} \right|^2. \quad (\text{S4})$$

B. Aberration correction

A simple way of taking the system aberrations into account is to consider that they can be modelled by a single phase mask in the pupil plane of the microscope objective. With the concern of not increasing the ill-posedness of the problem, we restrain the aberration mask to a linear combination of a few even polynomials ($N_a \leq 8$) in the Fourier domain:

$$\Phi_k(f_x) = \begin{cases} \sum_{p=1}^{N_a} \alpha_p \left(f_x - \frac{n_0 \sin \theta_k}{\lambda} \right)^{2p} & \text{if } |f_x| \leq \frac{\text{NA}}{\lambda} \\ 0 & \text{otherwise,} \end{cases} \quad (\text{S5})$$

where f_x refers to the 1D Fourier domain variable, NA is the numerical aperture of the objective lens and $\{\alpha_p\}_{1 \leq p \leq N_a}$ are unknown coefficients to be optimized along with ΔRI . We note that in order to be consistent with the propagation method defined in S1 we also have to translate the aberration mask according to the incoming wave angle.

The previous forward model can simply be extended by applying the following operator to the final field distribution $E_k|_{z=L_z}$ before computing its intensity:

$$\mathcal{A}_{\Phi}(E_k) = \mathcal{F}^{-1} \left(\mathcal{F}(E_k) e^{i\Phi_k} \right). \quad (\text{S6})$$

The result of the forward model becomes:

$$I_{\text{sim}}^{(k)} = \left| \mathcal{A}_{\Phi} \left(E_k|_{z=L_z} \right) \right|^2. \quad (\text{S7})$$

3. ERROR DISTANCE AND GRADIENT BACKPROPAGATION

We pose the RI reconstruction problem as the joint minimization of the l_2 distances between the experimental and simulated intensities:

$$\begin{aligned} e &= \frac{1}{N} \sum_{k=1}^N \|I_{\text{sim}}^{(k)} - I_{\text{exp}}^{(k)}\|_2^2 \\ &= \frac{1}{N} \sum_{k=1}^N \int \left(I_{\text{sim}}^{(k)}(x) - I_{\text{exp}}^{(k)}(x) \right)^2 dx. \end{aligned} \quad (\text{S8})$$

We can derive the expressions of the gradients of the error e with respect to $\Delta\text{RI}(x, z)$ and $\{\alpha_p\}_{1 \leq p \leq N_a}$ by following the algorithmic differentiation rules presented in [3]. In the following, we also employ the overbar notation to denote these gradients.

To do so, we first introduce the error-field E_k^{err} associated to the field E_k by:

$$\begin{aligned} E_k^{\text{err}} &= \overline{\mathcal{A}_\Phi \left(E_{k|z=L_z} \right)} \\ &= \frac{4}{N} \left(I_{\text{sim}}^{(k)} - I_{\text{exp}}^{(k)} \right) \mathcal{A}_\Phi \left(E_{k|z=L_z} \right). \end{aligned} \quad (\text{S9})$$

From E_k^{err} defined in S9, we can immediately derive the gradients $\{\overline{\alpha_p}\}_{1 \leq p \leq N_a}$:

$$\overline{\alpha_p} = \int \sum_{k=1}^N \left(f_x - \frac{n_0 \sin \theta_k}{\lambda} \right)^{2p} \Im \left\{ \left(\mathcal{F} \left(E_{k|z=L_z} \right) \right)^* e^{-i\Phi_k} \mathcal{F} \left(E_k^{\text{err}} \right) \right\} df_x. \quad (\text{S10})$$

Finally, we can successively compute the backpropagated gradients $\overline{\Delta\text{RI}}(x, l_z)$ with $l_z = \frac{\Delta z}{2} + (N_l - 1 - l)\Delta z$ for $l \in \{0, \dots, N_l - 1\}$, by applying the hermitian adjoints of the operators defined in S3:

$$\overline{\Delta\text{RI}}(x, l_z) = \sum_{k=1}^N \frac{2\pi}{\lambda} \frac{\Delta z}{\cos \theta_k} \Im \left\{ E_{k|z=l_z}^* \left(\mathcal{P}_{\Delta\text{RI}}^{(l)} \circ \mathcal{P}_{\frac{\Delta z}{2}}^* \circ \mathcal{A}_\Phi^\dagger \right) \left(E_k^{\text{err}} \right) \right\}. \quad (\text{S11})$$

4. ITERATIVE ALGORITHM

The reconstruction algorithm can be formulated as a minimization of the error distance defined in S8, according to the spatial ΔRI distribution and the aberration coefficients $\{\alpha_p\}$. Such minimization is typically achieved through a gradient descent. In order to deal with the missing cone problem, due to a limited range of illumination angles, and to recover from noisy experimental data, we add a regularization term to the error distance. The regularized minimization problem reads as:

$$\min_{\Delta\text{RI}, \{\alpha_p\}} \frac{1}{N} \sum_{k=1}^N \|I_{\text{sim}}^{(k)} - I_{\text{exp}}^{(k)}\|_2^2 + \kappa \|\Delta\text{RI}\|_{\text{TV}_l}, \quad (\text{S12})$$

where κ is a positive constant and $\|\cdot\|_{\text{TV}_l}$ designs the isotropic TV-norm [4], which is typical in tomographic reconstruction problems.

We perform the minimization S12 with a proximal gradient descent [4, 5] meant to take into account this regularization term in combination with the gradients already computed in S10 and S11. Eventually, we implement a convergence acceleration thanks to the classical Nesterov's momentum algorithm [6, 7].

REFERENCES

1. M. Feit and J. Fleck, "Light propagation in graded-index optical fibers," *Appl. Opt.* **17**, 3990–3998 (1978).
2. Y. Bao and T. K. Gaylord, "Clarification and unification of the obliquity factor in diffraction and scattering theories: discussion," *JOSA A* **34**, 1738–1745 (2017).
3. A. S. Jurling and J. R. Fienup, "Applications of algorithmic differentiation to phase retrieval algorithms," *JOSA A* **31**, 1348–1359 (2014).
4. A. Beck and M. Teboulle, "Fast gradient-based algorithms for constrained total variation image denoising and deblurring problems," *IEEE Transactions on Image Process.* **18**, 2419–2434 (2009).

5. N. Parikh and S. Boyd, "Proximal algorithms," *Foundations Trends Optim.* **1**, 127–239 (2014).
6. Y. E. Nesterov, "A method for solving the convex programming problem with convergence rate $o(1/k^2)$," in *Dokl. akad. nauk Sssr*, vol. 269 (1983), pp. 543–547.
7. A. Beck and M. Teboulle, "A fast iterative shrinkage-thresholding algorithm for linear inverse problems," *SIAM J. on Imaging Sci.* **2**, 183–202 (2009).